Data in Brief 57 (2024) 110986

Contents lists available at ScienceDirect

Data in Brief

journal homepage: www.elsevier.com/locate/dib

Data Article

# Multiproxy quantitative paleoceanographic dataset from late Quaternary marine sediment archives in the western Ross Sea (Antarctica)

Fiorenza Torricella[a], Ester Colizza[b,*], Gianluca Cornamusini[c], Paola Del Carlo[d], Federico Giglio[a], Jong Kuk Hong[e], Boo-Keun Khim[f], Gerhard Kuhn[g], Patrizia Macrì[h], Elisa Malinverno[i], Romana Melis[b], Leonardo Sagnotti[h], Bianca Scateni[d], Mirko Severi[j], Rita Traversi[j], Kyu-Cheul Yoo[e], Luca Zurli[c], Lucilla Capotondi[k]

[a] *Consiglio Nazionale delle Ricerche (CNR)-Istituto di Scienze Polari – ISP. Via P. Gobetti, 101, Bologna, Italy*
[b] *Università degli Studi di Trieste, Dipartimento di Matematica, Informatica e Geoscienze (MIGe), Via Weiss 2, Trieste, Italy*
[c] *Università di Siena, Dipartimento di Scienze Fisiche, della Terra e dell'Ambiente, via Laterino 8, 53100 Siena, Italy*
[d] *INGV - Istituto Nazionale di Geofisica e Vulcanologia - Sezione di Pisa, V. Battisti 53, 56125 Pisa, Italy*
[e] *Korea Polar Research Institute, Incheon 21990, South Korea*
[f] *Department of Oceanography, Pusan National University, Busan 46241, South Korea*
[g] *University of Bremen, Germany*
[h] *INGV - Istituto Nazionale di Geofisica e Vulcanologia -, Via di Vigna Murata 605, 00143 Roma, Italy*
[i] *Università di Milano-Bicocca, Dipartimento di scienze della Terra e Ambientali, Piazza della Scienza, 4, 20126 Milano, Italy*
[j] *University of Florence, Chemistry Dept. "Ugo Schiff", Via della Lastruccia, 3, 50019 Sesto Fiorentino, FI, Italy*
[k] *Consiglio Nazionale delle Ricerche (CNR)-Istituto di Scienze Marine – ISMAR, Via P. Gobetti, 101, Bologna, Italy*

ARTICLE INFO

*Article history:*
Received 6 May 2024
Revised 20 September 2024
Accepted 24 September 2024
Available online 28 September 2024

ABSTRACT

The past ice sheet dynamics and the timing of retreat events in the paleo-record in the Ross Sea is an issue still few understood. In order to contribute to this topic, we provide a multiproxy data from marine sediment archives (cores and box cores) collected in three sites in the Central Basin (Western Ross Sea, Antarctica). Each site recorded different environments, affected by different oceanographic conditions and

* Corresponding author.
*E-mail address:* colizzae@units.it (E. Colizza).
*Social media:* @Patrizia_Macri (P. Macrì), @leosagnotti (L. Sagnotti), @LucaZurli (L. Zurli)

https://doi.org/10.1016/j.dib.2024.110986

Dataset link: Dataset of sediment cores and box cores collected in Central Basin, Ross Sea (Antarctica) (Original data)

*Keywords:*
Central Basin
Paleomagnetism
Sedimentology
Grain size
Tephra
Chemistry
Micropaleontology

sedimentary regime. This makes the three investigated sediment cores and box cores unique and useful for comparison with other studied cores collected in the same basin. The data set includes physical (paleomagnetism, grain size and petrography), chemical, micropaleontological (diatom, foraminifera and silicoflagellate assemblages) analyses and cryptotephra characterization increasing the information already reported in literature. The importance of this dataset is related to a multi-disciplinary approach in a site, the Central Basin, few investigated which represents a key area to connect the Southern Ocean and the Ross Sea.



## Specifications Table

| | |
|---|---|
| Subject | Earth and Planetary Sciences-Geology |
| Specific subject area | *Paleoenvironmental evolution of the Central Basin (Western Ross Sea, Antarctica) during the Late Quaternary* |
| Type of data | *Table, Figure* |
| Data collection | Gravity sediment cores and box cores were collected by R/V Italica in 1998 and by IBRV Araon in 2013. Sedimentary material is stored at the Sorting Center—Trieste Section of the Museo Nazionale dell'Antartide<br>Paleomagnetism measurements were carried out using 2G Enterprises' DC 755 superconducting rock magnetometer (SRM). Grain size data were obtained by using the Malvern Mastersizer 2.0 particle analyzer.<br>Diatom and silicoflagellate abundances were obtained by counting the permanent slide using an LM microscope at 1000 X.<br>Foraminifera counts were made on sediment faction >63 μm using the stereomicroscope LEICA MZ 8. All dry residues are available at the CNR-ISMAR repository.<br>Sand and gravel petrography were carried out with the optical microscope Olympus BX51; modal classification of sand follows the Indiana point-counting method.<br>Tephra analyses were performed using *JEOL JXA-8200 electron microprobe (EPMA).*<br>Elemental concentration was obtained with *Avaatech X-ray fluorescence core scanner (XRF-CS) and ITRAX Core Scanner. Discrete samples where analysed by ICP-AES method.* |
| Data source location | Central Basin, Western Ross Sea, Antarctica.<br>Sediment core coordinates:<br>ANTA95-98C (72°32.87'S; 177°34.43'E; water depth of 1788m),<br>KI13-C1 (71° 51.9944'S; 179°30.3387'E; water depth of 2246m),<br>KI13-C2 (71°52.4758'S; 177°48.0854'E; water depth of 1800m).<br>Box core coordinates:<br>KI13-BC2 (71°21.00'S; 179°30.33' E; water depth of 2246 m)<br>KI13-BC3 (71°52.47'S; 177°48.08' E; water depth of 1800 m)<br>KI13-BC4 (72°32.87'S; 177°33.43' E; water depth of 1788 m) |
| Data accessibility | Dataset is in supplementary files (excel files).<br>Dataset is available in ZENODO.<br>https://zenodo.org/records/11091251<br>DOI: 10.5281/zenodo.11091251 |
| Related research article | *Torricella F., Melis R., Malinverno E., Fontolan G., Bussi M., Capotondi L., Del Carlo P., Di Roberto A., Geniram A., Kuhn G., Khim B-K., Morigi C., Scateni B. and Colizza E. Environmental and Oceanographic Conditions at the continental Margin of the Central Basin, Northwestern Ross Sea (Antarctica) Since the Last Glacial Maximum. Geosciences,* 11, *155, 2021* [1] |

## 1. Value of the Data

- This dataset provides new insight useful for decipher the glacial dynamic and evolution during the Late Pleistocene-Holocene periods in the Central Basin.
- The multiproxies sourced data may be used also for past climate/oceanographic models simulations in the north western Ross Sea.
- The data may be used in a wide range of paleoceanographic-paleoclimate based studies in the Antarctic region.

## 2. Background

Data are from two sediment cores and three box cores were collected during the KOPRI ANA03B cruise onboard the IBRV ARAON in February 2013 in the framework of the scientific collaboration between Italy and Korea (K-PORT and PNRA/ROSSLOPE Projects). In the framework of PNRA/ROSSLOPE project another sediment core collected in 1998 by R/V Italica was studied. These projects aimed to investigate the past glacial and oceanographic dynamics in the western Ross Sea continental margin area, specifically in the Central Basin [1–4] (Fig. 1). The basin is a deep semi-closed tectonic depression located along the north western margin of the Ross Sea continental shelf at the mouth of the JOIDES basin. This is a key area to investigate the bottom current behavior and Ross Ice Shelf activity during past glacial and interglacial periods. Oceanographic studies (i.e. [5]) indicate that the Warm Circumpolar Deep Water enters the Central Basin and mixes with High Salinity Shelf Water (HSSW). A branch of HSSW descends the continental slope through the JOIDES Basin forming the Antarctic Bottom Water (AABW).

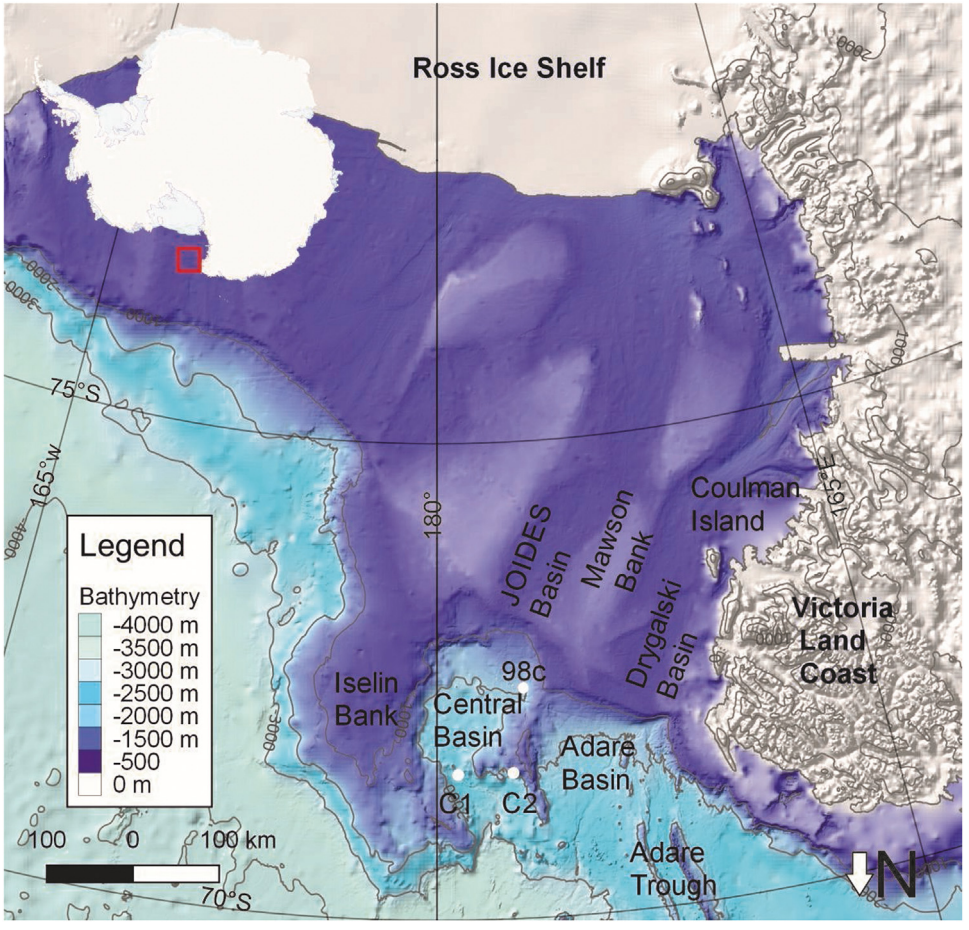


**Fig. 1.** Bathymetric map of the Ross Sea (modified from Arndt et al. 2013). White dots indicate the studied sediment cores: C1= KI13-C1 and -BC2, C2= KI13-C2 and BC3, 98c= ANTA95-98c and BC4.

## 3. Data Description

1. KI13-C1.xlsx is the dataset referred to the sedimentary core called KI13-C1 (Fig. 1) and consists of paleomagnetism, grain size data, petrographical analyses both on gravel and sand fraction, tephra characterization, chemical analyses including both XRF and ICP-AES, diatom, silicoflagellate and foraminifera data.
2. KI13-C2.xlsx is the dataset referred to the sedimentary core called "KI13-C1" (Fig. 1) and consists of paleomagnetism, grain size data, petrographical analyses both on gravel and sand fraction, chemical analyses including both XRF and ICP-AES. Diatom, foraminifera, and silicoflagellate data of core KI13-C2 from [3] are available here: https://jm.copernicus.org/articles/40/15/2021/jm-40-15-2021-supplement.pdf
3. ANTA95-98c.xlsx is the dataset referred to the sedimentary core called "ANTA95-98c" (Fig. 1), grain size data, petrographical analyses both on gravel and sand fraction, chemical analyses including both XRF and ICP-AES, diatom and foraminifera data.
4. KI13-BC2.xlsx is the dataset referred to the sedimentary box core called "KI13-BC2" (Fig. 1), grain size data, chemical analyses by ICP-AES, diatom and silicoflagellate data.

5. KI13-BC3.xlsx is the dataset referred to the sedimentary box core called "KI13-BC3" (Fig. 1), grain size data, chemical analyses by ICP-AES, diatom, silicoflagellate and foraminifera data.
6. KI13-BC4.xlsx is the dataset referred to the sedimentary box core called "KI13-BC4" (Fig. 1), gran size data, diatom, silicoflagellate and foraminifera data.
7. Radiocarbon dating.xlsx. This dataset consists of raw radiocarbon dating performed on the three sedimentary core and box-cores.

## 4. Experimental Design, Materials, Methods

### *4.1. Paleomagnetism*

The working sections of the C1 and C2 cores were subsampled with u-channel plastic holders for continuous paleomagnetic and rock magnetic analyses. Paleomagnetic and rock magnetic measurements were carried out using on small access (45 mm diameter) automated pass through '2G Enterprises' DC 755 superconducting rock magnetometer (SRM), installed in a magnetically shielded room and equipped with a set of three perpendicular coils for in-line orthogonal alternating field (AF) demagnetization. For each u-channel, we measured at 1 cm spacing both the low-field magnetic susceptibility (k) and the natural remanent magnetization (NRM); k was measured using a Bartington magnetic susceptibility meter equipped with probe MS2C and mounted in-line with the SRM translating system. The NRM was then subjected to a cycle of alternating field (AF) demagnetization in ten steps up to a maximum peak field of 100 mT (steps: 0, 5, 10, 15, 20, 30, 40, 50, 60, 80, and 100 mT). The NRM demagnetization data were analyzed using the DAIE workbook [5], computing the declination, inclination, and maximum angular deviation (MAD) of characteristic remanence components by principal component analysis on data measured from consecutive AF steps. Moreover, from the AF demagnetization curves we computed the median destructive field (MDF) of the NRM, defined as the value of peak AF required to reduce the remanence intensity to half of its initial value and used as a proxy for magnetic coercivity of the magnetic carriers. Finally, we also computed the $\Delta$GRM/$\Delta$NRM ratio, as a mean to quantify the tendency to acquire a spurious gyromagnetic remanent magnetization (GRM) at high AF demagnetization steps [6]. This parameter is considered a sensitive proxy for the occurrence of greigite ($Fe_3S_4$), an authigenic ferrimagnetic iron sulfide, that may form during a deposition under anoxic conditions as well as during late diagenesis, causing a remagnetization of the sediments [7].

#### *4.1.1. Grain size analysis*

The samples (ca. 3.0 g) were oven-dried at 50 °C, and each sample was placed in a beaker with about 2 mL of hydrogen peroxide (10 %) and distilled water and put on a hot plate for about 24 h. This treatment is useful to remove the organic matter that causes particle flocculation and to disaggregate the sample. Subsequently, the sediment was washed with distilled water through a 1 mm sieve. The passing sediment fraction was re-suspended using a magnetic stirrer, and an aliquot was taken with a pipette and dispersed in the sediment sampler of the Malvern MasterSizer 2000 laser. The instrumental data are then processed by a software program coupled with the Malvern size analyzer. The fraction major than 1 mm, was dried on a hot plate at 50 °C and separated through a 2 mm sieve. The fraction >1 mm and >2 mm was visually separately counted. Textural data were elaborated following the [8] classification and [9].

#### *4.1.2. Petrographic analysis*

Sieved samples derived from grain size analysis were used to define the compositional characterization of sediments using petrographic techniques. Samples were analysed with the optical microscope Olympus BX51. Both the gravel (>2 mm) and sand (<2 mm) fractions were mounted with epoxy and then petrographic thin sections were prepared. For the sand fraction, the modal classification was carried out following the Indiana point-counting method [10]. Eleven sand-sized samples were analysed from core 98c, 5 from core C1, and 7 from core C2. Most of the

samples, due to the small dimensions, do not allow the count of 300 grains per sample. A total of 21 samples were prepared from core 98c, 5 from core C1, and 18 from core C2. Every gravel-sized clast has been classified.

*4.1.3. Cryptotephra analysis*

Cryptotephra layers were initially identified based on significant peaks in the magnetic susceptibility prophile associated with indicative features shown by X-ray fluorescence (XRF) core scanning data. Samples were washed with deionized water in an ultrasonic bath to remove impurities, dried at 60°C, mounted with epoxy resin in 1-inch stubs, polished, and prepared for textural and geochemical analyses. The textures of glass particles and mineral phase composition were studied using a scanning electron microscope (SEM), Zeiss EVO MA. Major and minor element glass composition was determined using a JEOL JXA-8200 electron microprobe (EPMA) equipped with five wavelength-dispersive spectrometers at the High-Pressure High-Temperature (HPHT) Laboratory of INGV-Rome. Operating conditions were 15 kV accelerating voltage, 8 nA beam current, 5 mm probe diameter, and 10 and 5 s acquisition time for peak and background, respectively. Standards of glass were analysed to test data accuracy during the EPMA analyses. The trace element compositions of glass shards were determined using laser ablation inductively coupled plasma mass spectrometry (LA-ICP-MS) system. The analyses were performed with a Teledyne Photon Machine G2 laser ablation system coupled with a Thermo Fisher Scientific iCAP-Q quadrupole-based ICP-MS ([11] and reference therein). The operating conditions were optimised by analysing reference material ([12] and reference therein) NIST SRM 612 to provide maximum signal intensity and stability for the ions of interest while suppressing oxides formation (ThO+/Th+ below 0.5 %). The U/Th ratio was also monitored and maintained close to 1. The stability of the system was evaluated on $^{139}$La, $^{208}$Pb, $^{232}$Th, and $^{238}$U by a short-term stability test. It consisted of 5 acquisitions (one minute each) on a linear scan of NIST SRM 612 glass reference material ([11] and reference therein). Tephra glasses were analysed using a circular laser beam with a diameter of 15 µm, 25 µm (NN15), a frequency of 8 Hz, and an energy density at the sample surface of 3.5 J/cm$^2$. NIST SRM 610 reference material ([12] and reference therein) was used as the calibrator, and $^{29}$Si as the internal standard. USGS BCR2G reference material was analysed as unknown to provide quality control ([12] and reference therein). Under these operating conditions, precision and accuracy are better than 10 % for all the investigated elements ([11] and reference therein).

*4.1.4. Chemistry*

XRF-CS and ICP AES were performed on sediment cores KI13-C1 and KI13-C2. An ITRAX Core Scanner (Cox Analytical Systems, Gothenburg, Sweden) with a sampling interval of 0.7 mm resolution where used to determine the elemental composition on half sediment cores.

Discrete samples were analysed by ICP AES method. An amount of about 50 mg of samples was put into a PFA vessel for the following microwave assisted mineralization.

The acidic mixture used to dissolve the sediment samples was composed of 8 mL of ultrapure $HNO_3$ obtained by sub-boiling distillation, 1.0 mL of suprapur HCl, and 1 mL of HF. The closed vessels were heated in a microwave oven (MarsXpress, CEM) using a 30 min temperature ramp to 205 °C. This temperature was then maintained for 90 min. After this step, the vessels were cooled before the addition of 6.0 mL of a saturated solution of suprapur $H_3BO_3$. The obtained solutions were then heated again to 205 °C using a ramp of 20 min and this temperature was kept for 20 additional minutes. The final solutions were finally diluted to a volume of 25.0 mL with ultra-pure water (resistivity $>$ 18MΩ; Milli-Q IQ 7003, by Merck-Millipore) and analysed using an ICP-OES. This method allowed a recovery close to 100 % for all the measured elements using MESS-3 as Reference Material. An amount of 5 mL of each sample was spiked with 100 µL of a 50 mg L$^{-1}$ Ge solution used as an internal standard. The concentration of the elements was determined in triplicate by a Varian 720-ES inductively coupled plasma atomic emission spectrometer (ICP-OES – axial view). The sample introduction system was set up using a concentric pneumatic nebulizer and a cyclonic spray chamber. Calibration standards were prepared daily by gravimetric serial dilution from commercial stock standard solutions of 1000 mg L$^{-1}$ of

each element. The operating conditions (gas flows, sample uptake, detector position, etc.) were adjusted to obtain the maximum signal intensity. A solution composed of 2 % v/v of $HNO_3$ was used between each sample to fully rinse the sample line to avoid memory effects.

XRF-CS element analyser and XRF on glass beads were performed on sediment core ANTA05-98c. In particular, the half sediment cores were measured with an Avaatech X-ray fluorescence core scanner (XRF-CS) with a sampling interval of 1 cm and spot size of 1 $cm^2$. These measurements (elemental peak counts) are semiquantitative only and highly determined by matrix effects of the split core surface (holes = air below the landing prism, humidity, grain size). Some of the elements detected are system immanent and generated by the rhodium (Rh) target material of the X-ray tube, or by the Ag-collimator of the detector. The intensity of Compton scattering of the X-ray beam is related to the water content of sediment core, therefore higher Ag counts from the collimator correlate with higher peak area Cl and Br XRF counts emitted from the salty porewater. They therefore often indicate as well higher biogenic opal content in the sediment as G. Kuhn detected in the ANDRILL ANT-2a core [13]. To demonstrate, for example, the variation of Fe to other elemental peak counts the log-normalized ratio of Fe counts to individual other elemental peak counts or the sum of Ti, Zr, K, and Si (or the sum of all collected) areal peak counts could be calculated [14,15].

An amount of 1.5 grams of grinded sample material were mixed with 6.5 grams of $Li_2B_4O_7$ and melted in an EAGON 2 (PANalytical) for the preparation of glass beads. These were measured with a wavelength dispersive AXIOS 1kW X-ray fluorescence (XRF) spectrometer (PANalytical). Results were obtained using the standardless OMNIAN and the synthetic wide-range oxide standards WROXI methods used at AWI. Results could be used to calibrate the semi-quantitative XRF-CS results.

*4.1.5. Micropaleontological analyses*

*4.1.5.1. Foraminifera counting.* Samples for foraminifera analyses were weighed, oven-dried at 50 °C and gently washed with distilled water through 63 µm sieve mesh. Calcareous and agglutinated tests count was carried out under a binocular stereomicroscope Leica MZ8 over the > 63 µm size fraction considering only well preserved specimens. For all samples the amount (g) of sediment analyzed was indicated. The taxa were identified at species levels following the Antarctic foraminiferal taxonomy reported in [3,15,16].

*4.1.5.2. Diatom Slide Preparation and counting.* Diatom slide preparation followed the technique described in Torricella et al. [2]. The samples (max 0.5 g) were oven-dried at 50 °C and each sample was placed in a beaker with 60 mL of 35 % hydrogen peroxide ($H_2O_2$), 40 mL of distilled water, and 0.5 g of anhydrous tetrasodium pyrophosphate ($Na_2H_2P_2O_7$). This solution removes the organic matter and disaggregates the sample including diatom's valve separation. Then, the beakers were placed on a hot plate (70 °C) for 45 min to remove all organic matter. A coverslip was placed inside a petri-dish and a known volume of solution was pipetted into a petri dish together with distilled water to obtain a homogeneous distribution of diatom on the coverslip. Drainage of the exceeding water contained in the petri-dish was removed utilizing an immersion cotton thread in the petri-dish for 10–20 h.

Then, the coverslips were glued to a microscope slide using the Norland Optical Adhesive 61 (NOA61) and dried for 15 minutes under UV light. Diatoms slides were counted using a microscope at 1000 × magnification (x l00 oil immersion objective and × l0 eyepieces) adding the ZEISS immersion oil (Immersol oil 518). At least 300 diatom valves were counted and identified in each slide at the species level. When diatom abundance was scarce and it was not possible to reach a count of 300 valves, 500 fields of view were observed. We used the counting procedures suggested by [17,18]. The absolute diatom abundance (ADA) in terms of number of valves per grams of dry sediments (nv/gds), was determined for each sample following the method described by Armand [17].

*4.1.5.3. Silicoflagellates slide preparation and counting.* Diatom slides were scanned for silicoflagellates at 200 magnification, counting 50-60 specimens of *Stephanocha speculum* to calculate ab-

solute silicoflagellate abundance using the formula proposed by [17]. When silicoflagellates are scarce, a slide surface up to 250 $mm^2$ was scanned. Each specimen of *S. speculum* was observed at 1000x to recognize the different morphotypes, following the taxonomic rules of Malinverno [19].

## Limitations

None.

## Ethics Statement

The authors confirm that the current work does not involve human subjects, animal experiments, or any data collected from social media platforms.

## CRediT Author Statement

Conceptualization: FT and EC; Data Curation FT (diatom slide preparation, identification, and counting), EC (grain size analyses); GC and LZ (petrographic analyses); LC and RM (foraminifera samples, identification, and counting), PDC and BS (cryptotephra analysis); FG (magnetic susceptibility); PM and LS (paleomagnetism); EM (silicoflagellate identification and counting); MS and RT (ICP-AES analyses), GK and KCY (XRF core scanner measurements). Writing - Original Draft: all authors, Writing - Review & Editing: all authors. Project administration: EC, Funding acquisition: EC and BKK.

## Declaration of Competing Interest

The authors declare that they have no known competing financial interests or personal relationships that could have appeared to influence the work reported in this paper.

## Data Availability

Dataset of sediment cores and box cores collected in Central Basin, Ross Sea (Antarctica) (Original data) (ZENODO).

## Acknowledgments

We thank the technicians, captain, and crew of IBRV Araon for their efforts in obtaining sediment samples and geophysical data during the ANA03B expedition. We would like to thank the Italian PNRA (Progetto Nazionale di Ricerca in Antartide) and KOPRI (Korean Polar Research Institute) for funding the campaign. This research used samples provided by the Sorting Center—Trieste Section of the Museo Nazionale dell'Antartide—and it was developed in the framework of the STREAM Project (Late Quaternary evolution of the ocean-ice sheet interactions: the record from the Ross Sea continental margin (Antarctica). EC and BK wish to express their appreciation to the Italian Ministry of Foreign Affairs and International Cooperation (MAECI PGR 00822 and 01060) and PNRA project (2010/A2.07), and the National Research Foundation of Korea (2019K1A3A1A25000116), Korea Institute of Marine Science & Technology (Ministry of Oceans and Fisheries: RS-2023-00256330 and KOPRI (Korea Polar Research Institute) project

(PE24090), respectively. This paper was funded by the University of Trieste (D86-FRA-2024 CUP J93C24000260005).

## References

[1] S. Kim, L. De Santis, J.K. Hong, E. Colizza, S. Kim, A. Bergamasco, S.-H. Lee, S.-G. Kang, M.K. Lee, H. Kim, Y. Choi, A. Geniram, H.G. Choi, J.I. Lee, K.-C. Yoo, Y. Park, Hunting paleoceanographic archives of ice sheet-ocean interaction in the northwestern Ross Sea, Antarctica, Front. Earth Sci. 11 (2023) 1234347, doi:10.3389/feart.2023.1234347.

[2] F. Torricella, R. Melis, E. Malinverno, G. Fontolan, M. Bussi, L. Capotondi, P. Del Carlo, A. Di Roberto, A. Geniram, G. Kuhn, B-K. Khim, C. Morigi, B. Scateni, E. Colizza, Environmental and oceanographic conditions at the continental margin of the central Basin, Northwestern Ross Sea (Antarctica) since the last glacial maximum, Geosciences 11 (2021) 155, doi:10.3390/geosciences11040155.

[3] R. Melis, L. Capotondi, F. Torricella, P. Ferretti, A. Geniram, J.K. Hong, G. Kuhn, B-K Khim, S. Kim, E. Malinverno, K.C. Yoo, E. Colizza, Last Glacial Maximum to Holocene paleoceanography of the northwestern Ross Sea inferred from sediment core geochemistry and micropaleontology at Hallett Ridge, J. Micropalaeontol. 40 (2021) 15–35, doi:10.5194/jm-40-15-2021.

[4] B.K. Khim, E. Colizza, J.I. Lee, F. Giglio, S. Ha, Y.S. Bak, Biological productivity and glaciomarine sedimentation in the Central Basin of the northwestern Ross Sea since the last glacial maximum, Polar Sci. 28 (2021) 100682, doi:10.1016/j.polar.2021.100682.

[5] L. Sagnotti, Demagnetization Analysis in Excel (DAIE)—an open source workbook in Excel for viewing and analyzing demagnetization data from paleomagnetic discrete samples and u-channels, Ann. Geophys. 56 (2013) D0114, doi:10.4401/ag-6282.

[6] Y. Fu, T. von Dobeneck, C. Franke, D. Heslop, S. Kasten, Rockmagnetic identification and geochemical process models of greigite formation in Quaternary marine sediments from the Gulf of Mexico (IODP Hole U1319A), Earth Planet. Sci. Lett. 275 (3-4) (2008) 233–245, doi:10.1016/j.epsl.2008.07.034.

[7] L. Sagnotti, A. Cascella, N. Ciaranfi, P. Macrì, P. Maiorano, M. Marino, J. Taddeucci, Rock magnetism and paleomagnetism of the Montalbano Jonico section (Italy): evidences for a late diagenetic growth of greigite and implications for magnetostratigraphy, Geophys. J. Int. 180 (2010) 1049–1066, doi:10.1111/j.1365-246X.2009.04480.x.

[8] G.M. Friedman, J.E. Sanders, in: Principles of Sedimentology, Wiley, New York, NY, USA, 1978, p. 792.

[9] R.L. Folk, W.C. Ward, Brazos River bar: a study in the significance of grain size parameters, J. Sediment. Res. 27 (1957) 3–26.

[10] L.J. Suttner. Sedimentary petrographic provinces: an evaluation. In: Ross, C.A. (Ed.), Paleogeographic Provinces and Provinciality. vol. 21 (1974). Society for Sedimentary Geology Special Publication, pp. 75–84.

[11] M. Petrelli, D. Morgavi, F. Vetere, D. Perugini, Elemental imaging and petro-volcanological applications of an improved Laser Ablation Inductively Coupled Quadrupole Plasma Mass Spectrometry, Periodico di Mineral. 85 (1) (2016), doi:10.2451/2015PM0465.

[12] K.P. Jochum, J. Pfänder, J.D. Woodhead, M. Willbold, B. Stoll, K. Herwig, M. Amini, W. Abouchami, A.W. Hofmann, MPI-DING glasses: new geological reference materials for in situ Pb isotope analysis, Geochem. Geophys. Geosyst. 6 (10) (2005), doi:10.1029/2005GC000995.

[13] M. Taviani, M. Hannah, D. Harwood, S.E., Ishman; K. Johnson, M. Olney, C. Riesselman, E. Tuzzi, R. Askin, A.G., Beu; S. Blair, V. Cantarelli, A. Ceregato, S. Corrado, B. Mohr, S.H.H. Nielsen, D. Persico, S. Petrushak, J. Raine, S. Warny, Palaeontological characterisation and analysis of the AND-2A core, ANDRILL Southern McMurdo Sound Project, Antarctica. In: TERRA ANTARTICA. - ISSN 11228628. - 15:1-2(2008), pp. 113–146.

[14] G.J. Weltje, R. Tjallingii, Calibration of XRF core scanners for quantitative geochemical logging of sediment cores: theory and application, Earth Planet. Sci. Lett. 274 (2008) 423–438.

[15] G. Kuhn, C.-D Hillenbrand, S. Kasten, J.A. Smith, F.O. Nitsche, T. Friederichs, S. Wiers, W. Ehrmann, J.P. Klages, J.M. Mogollón, Evidence for a palaeo-subglacial lake on the Antarctic continental shelf, Nat. Commun. 8 (2017) 15591, doi:10.1038/ncomms15591.

[16] L. Capotondi, S. Bonomo, G. Budillon, P. Giordano, L. Langone, Living and dead benthic foraminiferal distribution in two areas of the Ross Sea (Antarctica), Rendiconti Lincei. Sci. Fisiche e Nat. 31 (4) (2020) 1037–1053, doi:10.1007/s12210-020-00949-z.

[17] L. Armand, The Use of Diatom Transfer Functions in Estimating Sea-Surface Temperature and Sea-Ice in Cores from the Southeast Indian Ocean Ph.D thesis, Australian National University, Canberra, Australia, 1997.

[18] X. Crosta, N. Koç, Diatoms: from micropaleontology to isotope geochemistry, in: C. Hillaire-Marcel, A. De Vernal (Eds.), Proxies in Late Cenozoic Paleoceanography, Developments In Marine Geology Series 1, Elsevier, Amsterdam, 2007, pp. 327–369.

[19] E. Malinverno, Extant morphotypes of Distephanus speculum (Silicoflagellata) from the Australian sector of the Southern Ocean: morphology, morphometry and biogeography, Mar. Micropaleontol. 77 (2010) 154–174, doi:10.1016/j.marmicro.2010.09.002.